JOURNAL OF MATERIALS SCIENCE **38** (2003) 1153–1159

Fatigue behaviour of beta Ti-22V-4Al alloy subjected to surface-microstructural modification

K. TOKAJI*
Department of Mechanical and Systems Engineering, Gifu University, 1-1 Yanagido, Gifu 501-1193, Japan
E-mail: tokaji@cc.gifu-u.ac.jp

S. TAKAFUJI
Department of Mechanical Engineering, Daido Institute of Technology, 10-3 Takiharu-cho, Minato-ku, Nagoya 457-0819, Japan

K. OHYA
Daido Castings Co. Ltd., 10 Ryugu-cho, Minato-ku, Nagoya 455-0022, Japan

Y. KATO
Gifu University, 1-1 Yanagido, Gifu 501-1193, Japan

K. MORI
Gifu University, 1-1 Yanagido, Gifu 501-1193, Japan

The present paper describes a surface-microstructural modification due to cold work and the fatigue behaviour of the surface-modified specimens in beta Ti-22V-4Al alloy. As-solution treated specimens were shot peened and then aged to achieve the modification. The obtained microstructure was first characterized and rotating bending fatigue tests were then performed using the surface-modified smooth specimens. The fatigue behaviour was evaluated and compared with the results of the conventional solution treated and aged specimens without modification. Surface-microstructural modification was successfully achieved within the region of 350 μm underneath the surface where hardness increased significantly compared with the core of the specimen, although there were some inhomogeneous precipitation areas in the modified region. The specimens without modification showed a step-wise *S-N* curve with the transition stress of approximately 600 MPa below which subsurface fracture occurred, while the surface-modified specimens did not exhibit step-wise *S-N* curve, but both surface-related and subsurface fractures took place up to a higher stress level of 720 MPa, leading to improved fatigue strength. In the surface-modified specimens, several facets were seen at the subsurface crack origin. The initiation sites were deeper than the specimens without modification, which corresponded to the inhomogeneous precipitation areas. The subsurface fracture process is further discussed on the basis of some mechanical approaches.

1. Introduction

Beta titanium alloys are considered as candidate for extensive applications to load-bearing structural components where fatigue properties are critical, because of their excellent properties such as strength to density, cold formability, weldability, and corrosion resistance [1]. Thus, there have recently been increasing interests in the fatigue behaviour of beta titanium alloys, but further studies are needed to realize the role of microstructural variables in various fatigue properties for establishing suitable microstructures and for contributing further material development, because a wide variety of microstructures can easily be produced with thermomechanical treatment. From such a viewpoint, the present authors have studied the effects of microstructure on fatigue properties in beta titanium alloys and indicated that microstructure exerted a significant influence on crack initiation and small crack growth behaviour [2–10].

In beta titanium alloys, very high strength can usually be obtained by ageing after solution treatment. In addition, it has been indicated that cold work enhanced significantly the ageing reaction during subsequent ageing process, because a number of lattice defects such as dislocations can be introduced to beta grains by cold work, which provide preferential nucleation sites of

*Author to whom all correspondence should be addressed.

alpha precipitates, leading to a further increase in strength [11–14]. When cold work is applied to the surface region of materials and then aged, one could obtain a surface microstructure modified material, because ageing reaction is highly intensified in plastically deformed surface region compared with the core of materials [15, 16].

In the present study, attempt was first made to achieve a surface-microstructural modification in beta Ti-22V-4Al alloy by using shot peening as one of cold working methods and rotary bending fatigue tests were then performed using the surface-modified smooth specimens. The fatigue behaviour was evaluated and compared with the results of the conventional solution treated and aged specimens.

2. Experimental procedures

2.1. Material

The material used in the present study is beta Ti-22V-4Al alloy of 26 mm diameter whose chemical composition (wt%) is V 22.6, Al 3.8, C 0.01, N 0.03, Fe 0.12, O 0.15, H 0.003. After solution treatment at 750°C for 1 h, fatigue specimens with a reduced diameter of 5.5 mm were machined. Subsequently, they were aged at 450°C for 8 h in order to prepare the conventional solution treated and aged specimens, hereafter designated as STA750. The mechanical properties of the specimens are tensile strength: 1279 MPa, elongation: 1%, reduction of area: 13%, and Vickers hardness: 380 [6, 7].

2.2. Surface-microstructural modification

In the present study, shot peening was employed as one of cold working methods to plastically deform the surface region. The thermomechanical process employed is shown in Fig. 1. Specimens solution treated at 750°C for 1 h were shot peened. The first stage of shot peening was performed with a relatively large arc height value of 0.608 mmA to produce a deep plastically deformed region. The second stage of the reduced arc height value of 0.300 mmA was used to minimize surface roughness. The resultant maximum roughness, R_y, of the specimens was 28.4 μm. Since surface roughness is detrimental to fatigue strength, particularly in titanium alloys, the shot peened specimens were mechanically polished by emery paper to completely remove the surface roughness. Subsequently, the same ageing treatment at 450°C for 8 h as STA750 was applied, by which residual stresses generated by shot peening were reduced to a negligible extent. By the process described above, changes in microstructure are expected to occur up to a certain depth underneath the specimen surface depending on the intensity of shot peening. The surface-modified specimens are designated hereafter as STA750M. Before fatigue experiment, both STA750 and STA750M were electropolished.

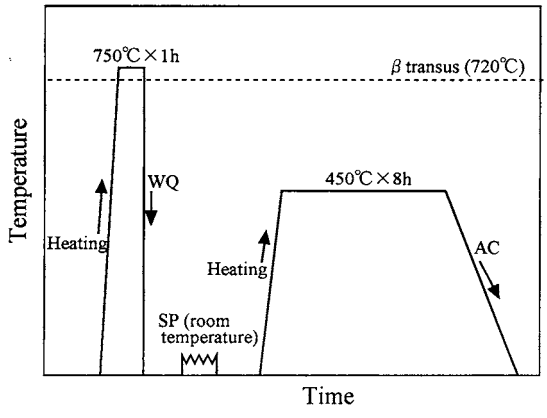

Figure 1 Thermomechanical treatment employed for surface-microstructural modification.

2.3. Procedures

Metallographic examination of microstructures was performed on the cross section of the specimens using both optical microscope and scanning electron microscope (SEM). Vickers hardness was also measured on the cross section with a load of 2.94 N. Fatigue tests were carried out using a 98 Nm capacity rotary bending fatigue testing machine operating at a frequency of 57 Hz in laboratory air at ambient temperature. After experiment, fracture surfaces were analyzed in detail using SEM.

3. Results

3.1. Microstructure characterization

Fig. 2 shows optical micrographs of the microstructures before and after ageing in the specimens subjected to shot peening. Before ageing (Fig. 2a), the microstructure consists of equiaxed beta grains. The grain structure within approximately 50 μm from the surface is not discernible because of heavy plastic deformation by cold work. Many slip bands and deformation twins are visible in beta grains in the subsequent region between 50 μm and 200 μm. In the region beyond 200 μm, the microstructure is the same as the core of the specimen. After ageing, i.e. in STA750M (Fig. 2b), the microstructure within 300 μm from the surface is different from the core. SEM micrographs of the aged microstructures are displayed in Fig. 3. In

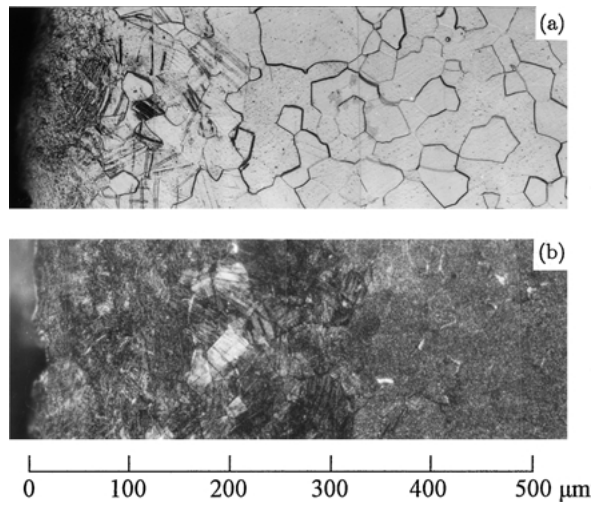

Figure 2 Optical micrographs of microstructures: (a) as-solution treated material, (b) material aged after shot peening (STA750M). Inhomogeneous precipitation areas are visible in (b) where they look white, particularly remarkable at approximately 200 μm from the surface.

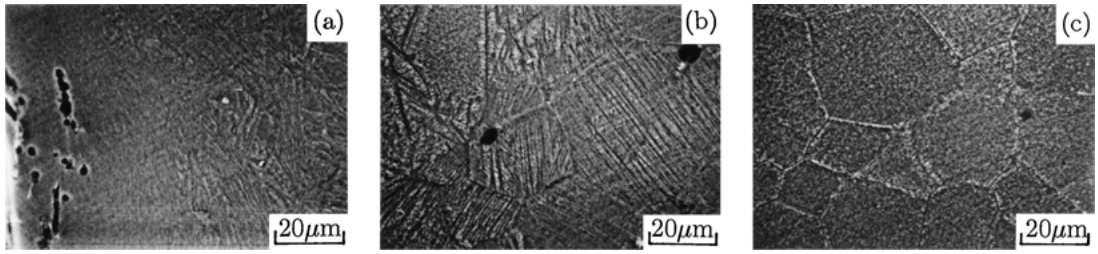

Figure 3 SEM micrographs of aged microstructures: (a) within 50 μm, (b) between 50 μm and 300 μm, and (c) beyond 300 μm from the surface. In (b), alpha phase is preferentially precipitated along slip bands produced by shot peening and thus between them precipitation is delayed.

the region deeper than 300 μm alpha precipitates are uniformly dispersed (Fig. 3c) and the microstructure is the same as the conventional solution treated and aged specimen, i.e. STA750. Fine alpha precipitates are generated in the near surface region (Fig. 3a). However, it should be noticed that some inhomogeneous precipitation areas can be recognized, where precipitation delays or takes place along slip bands and twins, particularly in the region between 150 μm and 300 μm (Fig. 2b, Fig. 3b).

Vickers hardness profile of STA750M is represented in Fig. 4 as a function of distance from the surface. Corresponding to the microstructure shown in Fig. 2b, hardness increases within the region of approximately 300 μm from the surface. It decreases with decreasing the distance from the surface and coincides with the core hardness that is almost the same as STA750. As described previously, surface roughness produced by shot peening was removed by polishing. Consequently, the fatigue specimen surfaces of STA750M are located between 70 μm and 110 μm from the surface shown in Fig. 2, which is indicated by gray band in Fig. 4.

Based on the above microstructure characterization and hardness measurement, it is concluded that surface-microstructural modification can be achieved by using shot peening, although some inhomogeneous precipitation areas were present in the surface-modified region.

3.2. Fatigue strength

The *S-N* curves of STA750M and STA750 are shown in Fig. 5. STA750 exhibits a definite step-wise *S-N* curve consisting of short life regime less than 10^5 cycles and long life regime more than 10^7 cycles. In the former region cracks initiated at the surface, while in the latter region, the crack initiation site was the interior of the specimens. The step-wise *S-N* curve results form different crack initiation mechanisms. As can be seen in the figure, the transition stress below which subsurface fracture takes place is approximately 600 MPa.

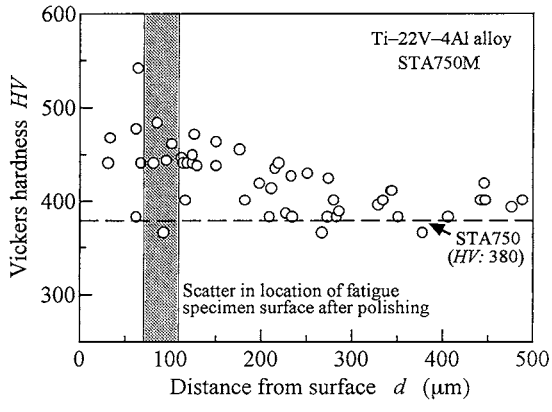

Figure 4 Vickers hardness profile for surface-modified material (STA750M).

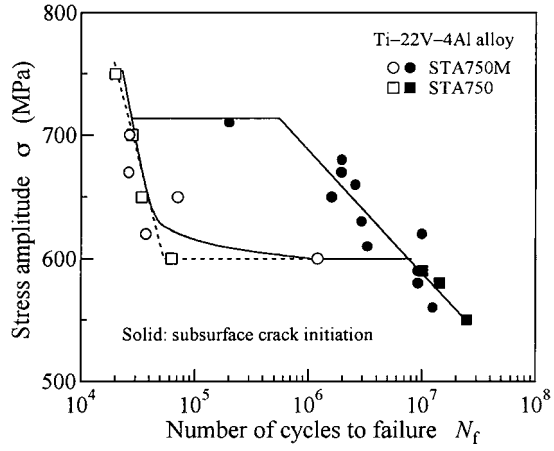

Figure 5 *S-N* diagram.

On the contrary, the surface-modified material, STA750M, does not show step-wise *S-N* curve, but both surface-related and subsurface fractures appear in the wide range of applied stress levels. For the surface-related fracture, fatigue lives are nearly the same as or longer than STA750, at higher stress levels and near the transition stress, respectively. For the subsurface fracture below the transition stress of 600 MPa of STA750, fatigue lives are identical because crack initiation and subsequent crack growth are not affected by surface-microstructural modification. However, it should be noted that the stress below which subsurface fracture occurs shifts to 720 MPa from 600 MPa, thereby fatigue lives increase significantly.

3.3. Fractography

SEM micrographs showing the crack initiation site in STA750 are displayed in Fig. 6. A facet was always seen in both surface-related and subsurface fractures, which appears to be related to grain boundaries [6]. Fig. 7 reveals SEM micrographs of the crack initiation site in STA750M. In surface-related fracture, a stage I facet can be seen (Fig. 7a), indicating that the crack generated by slip deformation in a beta grain. On the other hand, in subsurface fracture (Fig. 7b), the crack initiation site is 70 μm below the specimen surface where several facets are clearly recognized with many straight patterns on their surface. Similar appearance was observed in all the specimens that showed subsurface fracture.

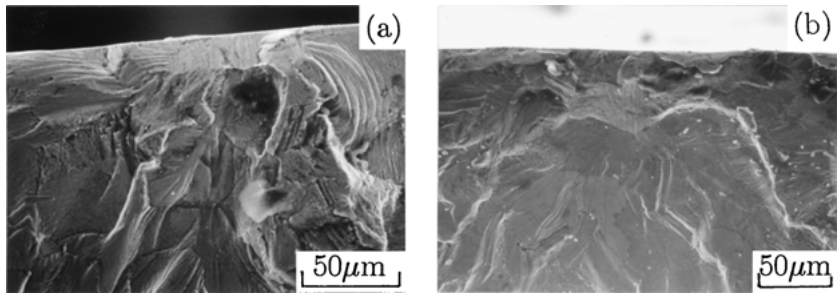

Figure 6 Examples of SEM micrographs showing crack initiation site in conventional solution treated and aged material (STA750): (a) surface-related ($\sigma = 650$ MPa, $N_f = 3.41 \times 10^4$) and (b) subsurface ($\sigma = 590$ MPa, $N_f = 1.01 \times 10^7$).

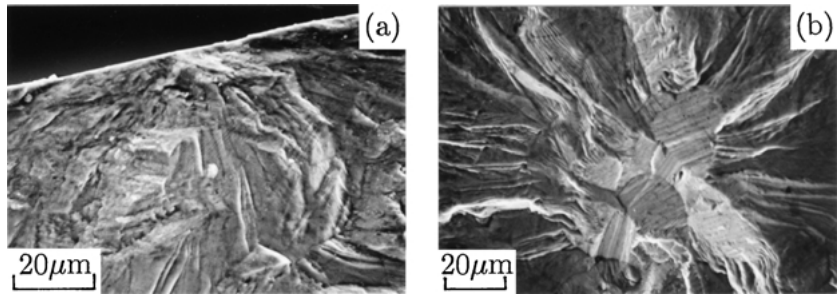

Figure 7 Examples of SEM micrographs showing crack initiation site in surface-modified material (STA750M): (a) surface-related ($\sigma = 700$ MPa, $N_f = 2.67 \times 10^4$) and (b) subsurface ($\sigma = 630$ MPa, $N_f = 2.95 \times 10^6$).

4. Discussion

4.1. Inhomogeneous precipitation in the modified microstructure

As shown in Figs 3 and 4, surface-microstructural modification was successfully achieved by ageing after shot peening. However, some inhomogeneous precipitation areas were seen in the region between 150 μm and 300 μm from the surface (Fig. 2b). Makino and Matsuda [17] have indicated that alpha phase was preferentially formed along slip lines produced by cold work and thus between them precipitation was delayed, leading to precipitation free zone. Fujii and Suzuki [18] have found similar delayed precipitation area in the microstructure that was plastically deformed by a punch followed by aged in a Ti-15V-3Cr-3Sn-3Al alloy. It was pointed out that dislocations and twin boundaries acted as the vacancy sinks rather than the precipitation sites. Difference in the extent of plastic deformation form grain to grain would be another reason for such an inhomogeneous precipitation structure.

As will be discussed later, such inhomogeneous precipitation areas seem to be related to the subsurface crack initiation in STA750M. Even in the region very close to the specimen surface, precipitation free zone are recognized (see Fig. 2b). Since the fatigue specimen surfaces of STA750M are located between 70 μm and 110 μm from the surface shown in Fig. 2, some specimens possibly have such inhomogeneous precipitation areas appeared on their surface. In such a case, surface-related fracture would take place, because cracks can easily initiate at the soft areas. The presence of the inhomogeneous precipitation areas is different in every specimen, thus it is believed that both surface-related and subsurface fractures coexisted in the wide range of applied stress levels as shown in Fig. 5.

4.2. Subsurface fracture promoted by surface-microstructural modification

Various surface modification techniques have been applied to engineering structural components for improvement in fatigue strength and wear resistance. In such surface-treated materials, subsurface fracture often occurs, because increased strength of the near surface region shifts the crack initiation site from the surface to the interior. Also in STA750M in the present study, hardness increased in the near surface region as seen in Fig. 4. Therefore, subsurface fracture took place up to a stress level that depends on both strength of near surface region and applied stress gradient.

As shown in Fig. 7b, several facets were always seen at the subsurface crack origin. The size and the distance from the surface to facet were measured. Square root of area of the facets projected onto the plane perpendicular to the specimen axis was employed as facet size. Fig. 8

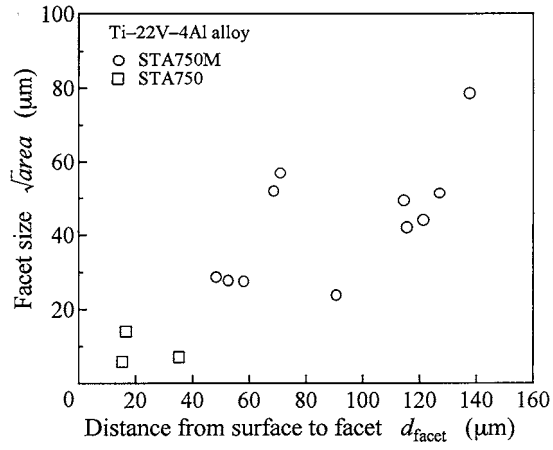

Figure 8 Relationship between facet size and distance from surface to facet.

shows the relationship between facet size and distance from the surface to facet. In this figure, the following points can be identified:

– subsurface crack initiation sites are much deeper in STA750M than in STA750,
– facet sizes are larger in STA750M than in STA750,
– facet sizes increase with increasing the distance from the surface to facet.

The subsurface crack origins in STA750M are between 50 μm and 140 μm from the fatigue specimen surface, i.e. between 120 μm and 250 μm from the surface after shot peening, which corresponds to the inhomogeneous precipitation areas (150 μm to 300 μm from the surface), from which subsurface fracture has started. In order to further establish the correlation of the subsurface crack initiation site with microstructure, additional fatigue tests have been conducted using specimens whose surface was removed by electropolishing by approximately 200 μm and 300 μm. These amounts of removal correspond to the inhomogeneous precipitation zone and the complete removal of the modified microstructure, respectively. The results are demonstrated in Figs 9 and 10. At the test stress level of 590 MPa, subsurface fracture was thought to occur independent

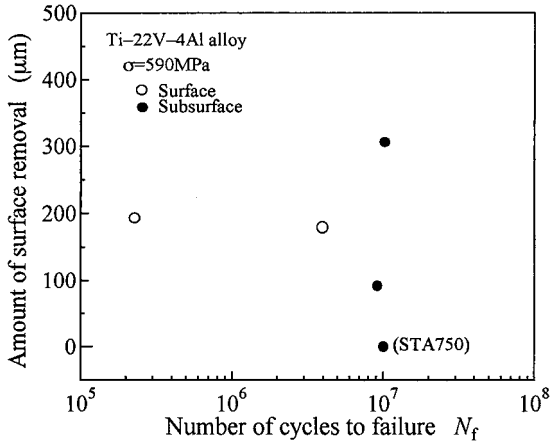

Figure 9 Fatigue test results of specimens whose surface was removed by electropolishing.

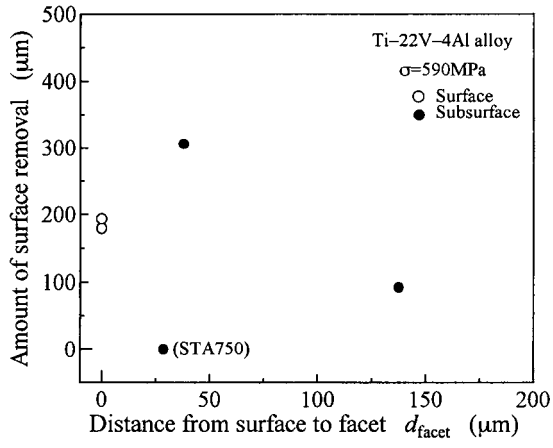

Figure 10 Distance from surface to facet for specimens whose surface was removed by electropolishing.

of the amount of removal (see Fig. 5), but the specimens with the amount of removal of 200 μm showed surface-related fracture. These results clearly indicate that the subsurface crack origin was closely related to the inhomogeneous precipitation areas in the modified microstructure as suggested in the previous section. Therefore, it is believed that subsurface cracks were generated by slip deformation within soft and weak grains in which precipitation delayed, because many straight patterns seen on the facet surface seem to be traces of slip deformation. As shown in Figs 9 and 10, the distance from surface to facet of the specimen with the amount of removal of 300 μm is nearly the same as that of STA750, which gives very reasonable result.

4.3. Mechanical approaches to subsurface fracture

The maximum stress intensity factor for facets observed in STA750M and STA750 was calculated using the following equation [19].

$$K_{max} = 0.5\sigma_{facet}\sqrt{\pi\sqrt{area}} \quad (1)$$

where σ_{facet} is the applied stress at the position of facets and $\sqrt{area}$ is the facet size. Fig. 11 shows the relationship between K_{max} and fatigue life. There is a considerable scatter, but fatigue life tends to increase as K_{max} decreases. This seems to imply that the process to facet formation, i.e. the crack initiation dominates the subsurface fracture process.

Using the crack propagation characteristic of STA750 that has already been obtained using CT specimens [8], the crack propagation life from facet size to final fracture was evaluated. Fig. 12 represents the crack propagation rate, da/dN, and stress intensity factor range, ΔK. The crack propagation law is given by the following equation.

$$\frac{da}{dN} = 1.83 \times 10^{-10}\Delta K^{2.633} \quad (2)$$

where da/dN and ΔK are in m/cycle and MPa$\sqrt{m}$, respectively. The crack propagation life was separated to

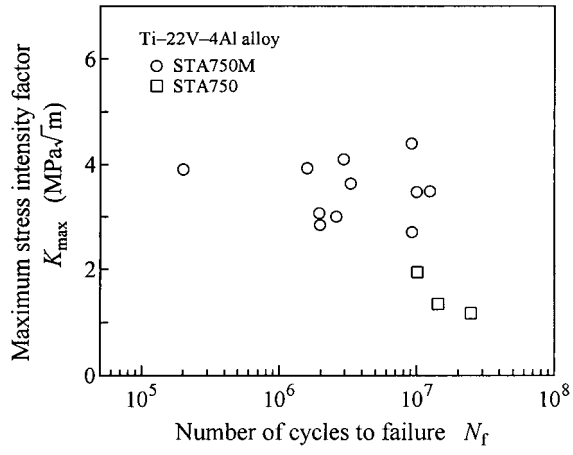

Figure 11 Relationship between maximum stress intensity factor for facets and fatigue life.

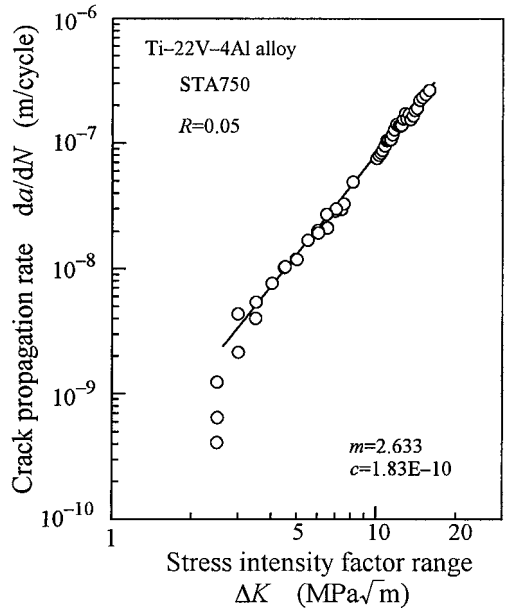

Figure 12 Relationship between crack propagation rate and stress intensity factor range for STA750.

two parts: the life from facet size to the size at which the internal crack reaches the surface and the subsequent life to final failure, for each of which ΔK was evaluated by the following equations [19].

$$\Delta K = 0.5\sigma\sqrt{\pi\sqrt{area}} \quad \text{for subsurface crack} \quad (3)$$

$$\Delta K = 0.65\sigma\sqrt{\pi\sqrt{area}} \quad \text{for surface crack} \quad (4)$$

The obtained results are listed in Table I. In both STA750M and STA750, the crack propagation lives are extremely small and almost negligible in all the specimens. Therefore, fatigue life is spent by either the facet generation life i.e. the crack initiation life or the life to the facet size from facet generation. Considering the very small facet sizes in STA750, it is thought that the former life dominates the fatigue life in subsurface fracture. The present estimation of crack propagation life relies on the following assumptions: cracks can propagate in the interior of the specimens according to Equation 2, and Equation 2 is applicable to small crack growth. Therefore, the obtained results are approximate, but coincide with the results that more than 99% of fatigue life was consumed by the crack initiation life [20]. Furthermore, it was confirmed by replication technique that in surface-related fracture of STA750, the crack initiation life was 70% to 80% of fatigue life [6] and the measured crack initiation lives in this case were in good agreement with the lives that subtracted the crack propagation lives estimated using the da/dN-ΔK relationship from the experimental fatigue lives.

TABLE I Calculated crack propagation lives in subsurface fracture

Material	σ (MPa)	N_f	N_p	N_c	N_c/N_f
STA750M	710	200300	6000	194300	0.97
	680	1975000	8800	1966200	0.996
	560	1951100	8600	1942500	0.996
	660	2594400	9000	2585400	0.997
	650	1598300	7100	1591200	0.996
	630	2945100	7400	2937700	0.998
	620	9989400	8800	9980600	0.999
	610	3302700	8700	3294000	0.997
	590	9180900	7700	9173200	0.999
	580	9220500	12800	9207700	0.999
	560	12434800	10900	12423900	0.999
STA750	590	10083800	8900	10074900	0.999
	580	14272600	13500	14259100	0.999
	550	24730000	14400	24715600	0.999

N_f: Experimental fatigue life.
N_p: Calculated crack growth life from facet size to failure.
N_c: Fatigue life to facet formation.

4.4. Improvement of fatigue strength by surface-microstructural modification

In STA750M, fatigue lives increased significantly because subsurface fracture took place up to a higher stress level than in STA750. In surface-related fracture, fatigue lives are almost the same as STA750, but tended to increase at lower stress levels near the transition stress (Fig. 5). From these results, it is concluded that fatigue strength can be improved by the surface-microstructural modification even though some inhomogeneous precipitation areas are present. If surface-microstructural modification are perfectly achieved without inhomogeneous precipitation area, then surface-related fracture would be suppressed, in other word, only subsurface fracture would occur up to a much higher stress level depending on stress gradient. As a result, fatigue strength would be greatly improved.

Finally, shot peening was employed as one of cold working methods in the present study, but it is not always a suitable method because surface roughness is produced. Instead, if a method that does not alter surface condition can be applied, then much better results would be expected in not only surface-microstructural modification, but also fatigue behaviour.

5. Conclusions

In this study, an attempt was first made to achieve surface-microstructural modification with ageing after shot peening in beta Ti-22V-4Al alloy. The fatigue behaviour of the surface-modified material was evaluated and compared with the conventional solution treated and aged material. The following conclusions can be made.

1. Surface-microstructural modification was successfully achieved within the region of 350 μm underneath the surface, where the hardness increased compared with the core of the specimens. However, some inhomogeneous precipitation areas were seen in the microstructure-modified region.

2. The conventional solution treated and aged material without modification (STA750) showed a stepwise *S-N* curve consisting of short life regime and long life regime, which was due to different crack initiation mechanisms: surface-related crack initiation and subsurface crack origin, respectively. The transition stress below which subsurface fracture occurred was approximately 600 MPa.

3. The surface-modified material (STA750M) did not show step-wise *S-N* curve, but both surface-related and subsurface fractures were seen up to a higher stress level of 720 MPa. In surface-related fracture, fatigue lives were similar to STA750 but increased slightly at lower stress level, while in subsurface fracture, they increased remarkably at the stress levels above the transition stress of STA750, but were almost the same below that stress level.

4. Several facets were always observed at the subsurface crack origin in the surface-modified material, which was different from STA750 in which only a small facet was seen. The surface-modified material showed much deeper crack initiation site and larger facet sizes than STA750 and the facet size increased as the initiation site became deeper.

5. The subsurface crack initiation sites corresponded to the inhomogeneous precipitation areas in the microstructure-modified region.

6. Based on the estimation of crack growth life using the crack propagation law, approximately 99% of fatigue life in subsurface fracture was occupied by the crack initiation process.

Acknowledgements

This work was financially supported by the Grant-in-Aid for Scientific Research ((C) No.12650079) of Japan Society for the Promotion of Science (JSPS). The authors wish to thank Mr Siraga for his experimental assistance.

References

1. P. J. BANIA, in "Beta Titanium Alloys in the 1990's" (TMS-AIME, Warrendale, PA, 1993) p. 3.
2. K. TOKAJI, J.-C. BIAN, T. OGAWA and M. NAKAJIMA, *Mater. Sci. Eng.* A **213** (1996) 86.
3. K. TOKAJI, H. SHIOTA and M. OHNISHI, *Tetsu-to-Hagane* **83** (1997) 281 (in Japanese).
4. K. TOKAJI, H. SHIOTA and J.-C. BIAN, *Mater. Sci. Eng.* A **243** (1998) 155.
5. K. TOKAJI and H. KARIYA, *ibid.* **281** (2000) 268.
6. K. TOKAJI, K.OHYA and H. KARIYA, *J. Soc. Mater. Sci., Japan* **49** (2000) 994 (in Japanese).
7. *Idem.*, *Fatigue Fract. Eng. Mater. Struct.* **23** (2000) 759.
8. *Idem.*, *Tetsu-to-Hagane* **86** (2000) 769 (in Japanese).
9. *Idem.*, in "Proc. Inter. Conf. Fatigue in the Very High Cycle Regime, Vienna, Austria, July 2001," edited by S. Stanzl-Tschegg and H. Mayer (University of Agricultural Sciences, Vienna) p. 141.
10. *Idem.*, *J. Soc. Mater. Sci., Japan* **50** (2001) 151 (in Japanese).
11. M. GUNSI, K. KITANO, N. NIWA and K. ITO, *Tetsu-to-Hagane* **72** (1986) 610 (in Japanese).
12. Y. OHTAKATRA, *Denkiseiko* **59** (1988) 87 (in Japanese).
13. N. NIWA, A. ARAI, H. TAKATORI and K. ITO, *ISIJ International* **31** (1991) 856.
14. Y. MOTOHASHI, E. IWAI, M. EBARA, T. SAKUMA and I. KUBOI, in Proc. 4th Japan Int. SAMPE Symposium, Tokyo, Japan, September 1995, edited by Z. Maekawa, E. Nakata and Y. Sakatani (Japan Chapter of SAMPE, Yokohama) p. 480.
15. A. BERG, J. KIESE and L. WAGNER, *Mater. Sci. Eng.* A **243** (1998) 146.
16. A. BERG, A. DRECHSLER and L. WAGNER, "Fatigue Behavior of Titanium Alloys" (TMS-AIME, Warrendale, PA, 1999) p. 267.
17. T. MAKINO and S. MATSUDA, in Proc. Int. Conf. Thermomechanical Processing of Steels and Other Materials, Wollongong, Australia, July 1997 (TMS, Warrendale, PA) p. 1519.
18. H. FUJII and H. G. SUZUKI, "Beta Titanium Alloys in the 1990's" (TMS-AIME, Warrendale, PA, 1993) p. 249.
19. Y. MURAKAMI, *Eng. Fract. Mech.* **22** (1985) 101.
20. R. CHAIT and T. S.DESISTO, *Metal. Trans.* A **8** (1977) 1017.

Received 29 May
and accepted 25 November 2002